Scientific African 19 (2023) e01489

Contents lists available at ScienceDirect

Scientific African

journal homepage: www.elsevier.com/locate/sciaf

# Application of ginger and grapefruit essential oil extracts on the corrosion inhibition of mild steel in dilute 0.5 M $H_2SO_4$ electrolyte

Roland Tolulope Loto[a,*], Moses M. Solomon[b]

[a] Department of Mechanical Engineering, Covenant University, Ota, Ogun State, Nigeria
[b] Department of Chemistry, Covenant University, Ota, Ogun State, Nigeria

ARTICLE INFO

*Article history:*
Received 18 June 2022
Revised 14 November 2022
Accepted 6 December 2022

Editor DR B Gyampoh

*Keywords:*
Carbon steel
Corrosion management
Essential oil
Inhibition
Environmental degradation

ABSTRACT

Admixture of ginger and grapefruit essential oils (GPP) were studied for their corrosion inhibition properties on mild steel (MS) in 0.5 M $H_2SO_4$ solution by potentiodynamic polarization, open circuit potential measurement, electrochemical impedance spectroscopy, weight loss analysis and ATF-FTIR spectroscopy. Results from potentiodynamic polarization shows GPP significantly reduced the corrosion of MS from 8.430 mm/y at 0% GPP concentration to values between 1.979 mm/y and 0.565 mm/y. The corresponding inhibition efficiency values ranged from 76.52% to 93.5% and corrosion current density from $1.88 \times 10^{-4}$ A/cm$^2$ to $5.36 \times 10^{-5}$ A/cm$^2$. GPP displayed mixed-type inhibition at all GPP concentrations studied. The OCP plot at 0% GPP initiated at -0.495V compared to -0.443V and -0.451V at 1% and 3.5% GPP. At 9000s, the corresponding OCP values are -0.442V, -0.410V and -0.424V due to electropositive plot shift and passivation of MS surface at 1% and 3.5% GPP, though significant potential transients were present on the OCP plot at 1% GPP. The electrochemical impedance results indicate that the corrosion resistance of MS increased from 4.402 Ω cm$^2$ to 99.318 Ω cm$^2$ upon the addition of 3.5% GPP resulting in inhibition efficiency of 96%. Data from weight loss analysis shows decrease in corrosion rate from 184.48 mm/y to values between 8.94 mm/y and 6.25 mm/y. The corresponding inhibition efficiency values varies from 95.16% at 1% GPP to 96.61% at 3.5% GPP concentration. The ATF-FTIR results confirm the adsorption of GPP molecules on the surface of the carbon steel electrode.



## Introduction

The economic value of carbon steels in addition to their versatile mechanical and physical properties accounts for their universal utilization in industrial and domestic environments worldwide [16]. They can be quenched, tempered, fabricated, welded and easily formed to desired specifications. Carbon steels combine strength with excellent ductility, hardenability

* Corresponding author.
*E-mail address:* tolu.loto@gmail.com (R.T. Loto).

https://doi.org/10.1016/j.sciaf.2022.e01489

and carburization properties. Utilization of carbon steels covers their usage as cold headed fasteners and bolts, shafts, sprockets, spindles, pins, crankshafts, couplings, rods and other high volume component devices. Carbon steel makeup 85% of the total steel production globally [34]. However, the steel is prone to significant damage resulting from corrosion [11,17,39]. The corrosion problem is due to the application of the steel in petrochemical, gas processing, automobile, construction, fertilizer production, desalination and extraction industries containing sulphates a major component of $H_2SO_4$ acid. This stems from the weak resistance of the steel to the electrochemical action of sulphates on the steel surface as a result of their inability to passivate within such environments. The oxide formed on the steel exhibits numerous pores enabling the electrolytic transport and diffusion of the corrosive species onto the substrate Fe. Passivating elements (Cr, Ni, Mo etc.) are responsible for the evolution of an impenetrable film and passivation on stainless steels [41]. $H_2SO_4$ acid is a universal commodity solution whose synthesis and production is an important reference point for a nation's industrial capacity. The solution is produced through a variety of techniques e.g. wet $H_2SO_4$ process, contact process etc. The acid is used in the production of fertilizers, petrochemical refining and production, chemical processing, production of dyes, batteries and bleaching agent, removal of metals from their ores and in rubber production [26,48,53]. The consequence of carbon steel corrosion in $H_2SO_4$ is high economic damage, decrease in operational lifespan, plant shutdowns, industrial accidents and enormous cost of repair and maintenance [1,4,63]. Corrosion prevention on carbon steels can be substantially reduced with customized corrosion control techniques that factors in the peculiarities of application and environmental conditions. Techniques such as such as surface modification, electrodeposition, electroplating, cathodic protection, paint coatings etc. have been proven to be effective but are limited in application and are costly. Fluid compounds identified as corrosion inhibitors have been proven to be effective, economical and versatile in corrosion prevention of carbon steels [47]. Although, corrosion inhibitors (i.e. inorganic and organic inhibitors) have been known for decades the confirmed effective ones have been shown to be toxic to the environment and personnel leading to restriction on their use by government regulations [12,36,40,42,57,66]. Green chemical compounds from plant extracts have shown promising corrosion inhibition characteristics. However, they tend to perform poorly, they are biodegradable, have short shelf life and lack strong adsorption performance on carbon steels [5,14,43,45,56]. Other results obtained from experimental investigations on green chemical compounds depict the importance of well documented repository inhibition effect, reactive species, effective functional lifespan and adsorptive properties [3,38,44,51,55]. Distillates from essential oils (plants, barks, seeds etc.) has been research into [8,10,18,19,24,30,37,45]. Results obtained by Znini [68], Bathily et al [69] and Hossain et al [31] from over two hundred published manuscripts on the corrosion performance of various essential oils extracts. showed that they performed effectively especially when related to their concentration and chemical properties. Nevertheless, the absence and toxic compounds in their natural forms, their abundance, renewability and environmental sustainability gives room for extensive research for corrosion inhibition. This also brings up the problem of documentation. One of the features of this article in addition to the problems earlier raised is to determine the threshold concentration for optimal performance of plant extracts. It's must be noted that essential oil distillates have been proven to be marginally effective but their corrosion inhibition effect highly dependent on concentration [13,15,46,60,61]. Fidrusli et al [22] studied the effect of ginger extracts and powder on the corrosion inhibition of mild steel in 1M HCl solution. Results showed inhibition efficiency increased with respect to ginger concentration with optimal inhibition efficiency of 91% and 86% from weight loss and polarization test. Narenkumar et al [50] studied the effect of ginger extract on the microbial (Bacillus thuringiensis EN2) corrosion resistance of mild steel in a cooling water system. The extract was observed to form a protective layer to prevent the biofilm formation. Maximum inhibition efficiency of 80% was obtained. Fouda et al [23] studied the effect of ginger extract on steel corrosion in sulfide polluted NaCl solution. Inhibition efficiency was observed to increase with inhibitor concentration with optimal value of 83.9% at 250 ppm of ginger. Gadow and Motawea [25] Studied the inhibitive effect of ginger roots extract on carbon steel corrosion in 1.0 M HCl solution at specific temperatures. Results showed inhibition efficiency increased with increase in concentration of the extract and decrease in temperature. Maximum inhibition efficiency of 94% at 200 ppm of extract and 25°C was attained. Batah et al [6] studied grapefruit oil extract as corrosion inhibitor on carbon steel in 1M HCl. Inhibiting action increased with extract concentration with highest efficiency of 86.15% at 1g/L of the extract. In support of the quest for effective green corrosion inhibitors for carbon steels, this research focusses on the protection effect of equal admixture ginger and grapefruit on mild steel in 0.5M $H_2SO_4$ solution. The purpose of the admixture is to study the synergistic effect of the two extracts and observed for significant variation in corrosion inhibition compared to their separate performances.

## Experimental methods

### *Materials and preparation*

Mild steel (MS) test sample with circular configuration of 1.2 cm diameter has elemental composition of 0.21% Cu, 0.29% Si, 1.04% Mn, 0.27% C, 0.06% S, 0.05% P and 98.08% Fe from energy dispersive spectroscopy analysis with PhenomWorld scanning electron microscope. The MS sample was divided into several smaller test samples with manual cutting tool into average dimensions of 1 cm length for weight loss measurement. MS test pieces for potentiodynamic polarization and open circuit potential analysis were attached to a Cu cable with lead before implanting in pre-hardened acrylic mixture. The visible surface of the steel was abraded with emery papers (60, 300, 600, 1000 and 1500 grits) and polished with 6 µm diamond fluid before washing with distilled $H_2O$ and propanone. Ginger and grapefruit (GPP) essential oil extracts were

purchased from NOW Foods, USA, and prepared in volumetric concentrates of 0%, 1%, 1.5%, 2%, 2.5%, 3% and 3.5% respectively per 200ml of 0.5M $H_2SO_4$ solutions at ratio 1:1.

*Potentiodynamic polarization and open circuit potential measurement*

Electrochemical analysis was carried out at 35 °C room temperature with a Digi-Ivy 2311 potentiostat (consisting of triple electrode configuration within a transparent beaker containing the acid-extract solution) and connected to a computer. The electrodes are MS electrodes with exposed surface area of 1.13 $cm^3$, Ag/AgCl standard electrode and Pt wire auxiliary electrode. Polarization plots were produced at scan rate of 0.0015 V/s from -1.1 V and +1.65 V. Corrosion current density $C_J$, ($A/cm^2$) and corrosion potential, $C_p$ (V) values were determined through Tafel derivation. Corrosion rate, $C_{RT}$ (mm/y) was computed from the mathematical relationship below;

$$C_{RT} = \frac{0.00327 \times C_J \times C_q}{D} \tag{1}$$

where $C_q$ is the correlative weight (g) of MS, 0.00327 is the corrosion constant and $D$ is density ($g/cm^3$). Inhibition efficiency, $I_{EF}$ (%) was calculated from below;

$$I_{EF} = \left[1 \; - - \left(\frac{C_{RT2}}{C_{RT1}}\right)\right] \times 100 \tag{2}$$

$C_{RT1}$ and $C_{RT2}$ are MS weight loss without and with the extracts. Polarization resistance, $P_R$, (Ω) was computed from below;

$$P_R = 2.303 \frac{B_a B_c}{B_a + B_c}\left(\frac{1}{I_{cr}}\right) \tag{3}$$

$B_a$ and $B_c$ are the anodic and cathodic Tafel slopes (V/dec). Open circuit potential measurements were performed at step potential of 0.2V/s for 9000 s in 0.5 M $H_2SO_4$ solution at 0%, 1% and 3.5% GPP concentration with the same electrode configuration as the potentiodynamic polarization test.

*Electrochemical impedance spectroscopy*

A Gamry Potentiostat/Galvanostat/ZRA Reference 600 + workstation was used for the electrochemical impedance spectroscopy (EIS) experiments. The experiments were carried utilizing the high carbon steel sample as the working electrode, a Ag/AgCl (sat. 4.2 M KCl) as the electrode, and a platinum rod as the counter electrode. Before the impedance characteristics of the working electrode were obtained, the open circuit potential was monitored for 1800 s. At the open circuit potential, the EIS measurements were performed under potentiostatic mode by applying an alternating–current signal with amplitude of 10 mV over a frequency range of 100,000 Hz to 0.1 Hz. The electrochemical impedance data obtained were analysed using the Echem analyst software.

*Weight loss measurement*

Weight of MS steel test pieces were determined and singularly suspended in 200 mL of the acid-extract solution for 240 h. MS weight determination was done at 24 h interval. Corrosion rate, $C_{RT}$ (mm/y) was determined from the relationship below;

$$C_{RT} = \left[\frac{87.6 W_L}{DAt}\right] \tag{4}$$

$W_L$ is the weight loss (g), $D$ is the density ($g/cm^3$), $t$ represents time (h), $A$ is the total exterior area of the MS specimen ($cm^2$) and 87.6 is the corrosion rate constant [35]. Inhibition efficiency ($\eta$) was determined from the following numerical expression below;

$$I_{EF} = \left[\frac{W_{L1} - W_{L2}}{W_{L1}}\right] \times 100 \tag{5}$$

$W_{L1}$ and $W_{L2}$ represents weight loss at specific extract concentrations.

*ATF-FTIR spectroscopy*

1% GPP concentration/0.5 M $H_2SO_4$ solution, before and following corrosion test were analysed under infrared particle emissions with Bruker Alpha FTIR (Fourier transform infrared spectroscopy) spectrometer within the wavelength span of 375 to 7500 $cm^{-1}$, and accuracy of 0.9 $cm^{-1}$ after 240 h of MS weight loss measurement. Spectral patterns were studied and linked to the conventional ATF-FTIR (Attenuated Total Reflectance-Fourier transform infrared spectroscopy) table. Tabulations were done for the reactive groups which influenced the redox reaction processes.

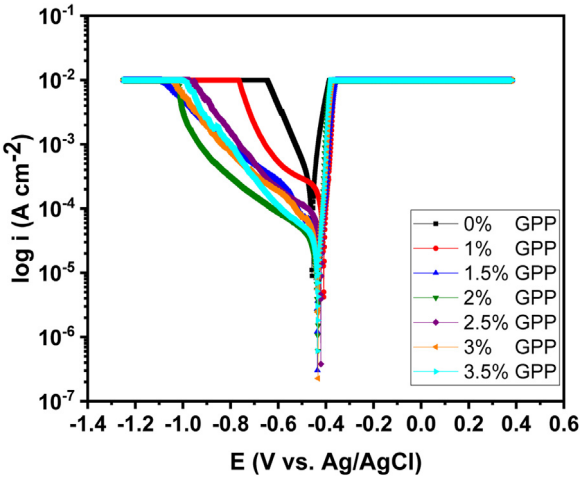


**Fig. 1.** Potentiodynamic polarization plots for MS corrosion in 0.5M $H_2SO_4$ solution at 0%-3.5% GPP concentration

**Table 1**
Potentiodynamic polarization data for MS corrosion in 0.5M $H_2SO_4$ solution at 0%-3.5% GPP concentration

| GPP Concentration (%) | MS $C_{RT}$ (mm/y) | GPP $I_{EF}$ (%) | Corrosion Current (A) | $C_J$ (A/cm$^2$) | $C_P$ (V) | $P_R$ (Ω) | $B_c$ (V/dec) | $B_a$ (V/dec) |
|---|---|---|---|---|---|---|---|---|
| 0 | 8.430 | - | 9.04E-04 | 8.00E-04 | -0.449 | 28.42 | -9.662 | 6.331 |
| 1 | 1.979 | 76.52 | 2.12E-04 | 1.88E-04 | -0.409 | 121.10 | -4.670 | 0.920 |
| 1.5 | 0.719 | 91.47 | 7.71E-05 | 6.83E-05 | -0.435 | 303.10 | -6.135 | 0.840 |
| 2 | 0.592 | 92.98 | 6.35E-05 | 5.62E-05 | -0.433 | 331.30 | -3.422 | 0.640 |
| 2.5 | 0.588 | 93.03 | 6.30E-05 | 5.58E-05 | -0.421 | 367.60 | -2.388 | 0.436 |
| 3 | 0.579 | 93.13 | 6.21E-05 | 5.49E-05 | -0.433 | 373.60 | -4.309 | 0.286 |
| 3.5 | 0.565 | 93.30 | 6.05E-05 | 5.36E-05 | -0.435 | 410.90 | -2.816 | 0.812 |

## Results and discussion

*Potentiodynamic polarization studies*

Cathodic and anodic polarization plots representing the corrosion polarization behavior of MS in 0.5 M $H_2SO_4$ solution at 1% - 3.5% GPP concentration are shown in Fig. 1. The polarization data retrieved from the plots are shown in Table 1. Observation of Table 1 shows MS corrosion rate value at 0% GPP concentration significantly varies from the corrosion rate at 1%-3.5% GPP concentration in relative manner compared to the observation from weight loss analysis. Corrosion rate at 0% GPP concentration is 8.430 mm/y corresponding to corrosion current density value of $8 \times 10^{-4}$ A/cm$^2$ and polarization resistance of 28.42 Ω. The corresponding polarization plot configuration shows significantly higher cathodic slope was observed compared to the anodic polarization slope which intersects at -0.449 V. The relatively higher cathodic and anodic polarization slope is due to accelerated cathodic reactions involving $O_2$ reduction and $H_2$ evolution, and anodic reactions involving surface oxidation of the steel [64]. However, beyond 0% GPP concentration significant decrease in the cathodic polarization slope was observed due to suppression of the cathodic half-cell reaction of the redox electrochemical process. In effect the cathodic processes were significantly slowed down with respect to GPP concentration. The anodic portion of the polarization varied marginally with respect to GPP concentration compared to the cathodic plots. This shows the anodic reactions are under activation control whereby increase in GPP concentration has limited influence on the anodic polarization behavior and inhibition of the steel. This is due to effective surface coverage of the steel irrespective of GPP concentration which will be further discussed in the weight loss measurement and optical microscopy section [47]. Addition of GPP extract to the acid solution shifts the corrosion potential of the polarization plot at all GPP concentrations positively relative to the corrosion potential at 0% GPP concentration. This signifies dominant anodic half-cell reaction within the overall redox reaction process [7]. However, the anodic shift is less than 85mV hence GPP inhibition mechanism is mixed-type [20]. Corrosion rate of MS significantly decreased in the presence of GPP extract from 8.430 mm/y at 0% GPP concentration to 1.979 mm/y at 1% GPP concentration and values ranging between 0.719 mm/y and 0.565 mm/y (1.5% -3.5% GPP concentration). Increased in GPP concentration marginally influenced the corrosion rate of MS after 1.5% GPP concentration. At 3.5% GPP concentration, optimal inhibition efficiency was attained at 93.3%, corresponding to corrosion current density of $5.36 \times 10^{-5}$ A/cm$^2$ and polarization resistance of 410.90 Ω.

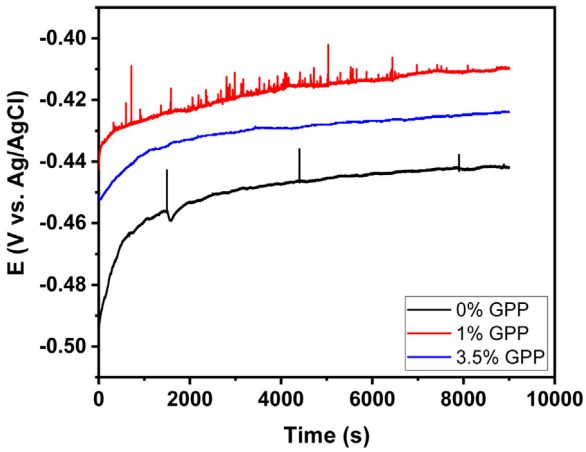


**Fig. 2.** OCP plots for MS in 0.5 M $H_2SO_4$ solution at 0%, 1% and 3.5% GPP concentration

*Open circuit potential analysis*

Open circuit potential (OCP)plots were produced for MS in 0.5 M $H_2SO_4$ solution at 0%, 1% and 3.5% GPP concentration for 9000s. The plots shown in Fig. 2 depict the active-passive transition behavior and thermodynamic properties of the surface characteristics of the steel at the metal-solution interface. The higher the corrosion rate of the steel i.e. redox electrochemical processes occurring on the steel surface. Hence, the more electronegative the plots relative to other plots [54]. The OCP plot at 0% GPP initiated at -0.495V compared to -0.443V and -0.451V for MS at 1% and 3.5% GPP concentration. The OCP plot sharply increased to electropositive values before attaining relative stability at 2019.82s (-0.453V). Beyond this point, the extent of variation of the thermodynamic properties of the steel becomes marginal till 9000s (-0.442V). The plot configuration shows that at initiation point the steel is exposed to the electrochemical action of the corrosive species i.e. the surface is in the active phase. Between 0s and 2019.82s, there is significant transition to passive phase and stable thermodynamic behavior. This is different from passivation in Cr based alloys. In carbon steels it simply refers to the point or region at which electrochemical deterioration of the steel attains equilibrium behavior even though corrosion still occurs throughout the exposure period. Addition of GPP extract at 1% and 3.5% GPP concentration shifted MS OCP plots to electropositive values signifying decreased redox reaction processes on the steel surface [59]. This is due to passivation of the steel through surface coverage by GPP extract as presented by optical microscopy analysis. The plots initiated at -0.443V and -0.451V (as earlier stated); however, the plot at 3.5% GPP concentration attained relative thermodynamic stability at 1600s (-0.434V) and culminated at -0.424V (9000s), though marginal shift to electropositive values was observed. The OCP plot at 1% GPP concentration remained thermodynamically unstable throughout the exposure hours with visible potential transient. It must be noted that the OCP plot at 1% GPP concentration is relatively more electropositive than the plot at 3.5% GPP concentration signifying decrease in corrosion reaction processes on the steel surface. However, despite effective protection of the steel surface, the surface properties of the steel are thermodynamically unstable resulting in the potential transients. This is due to instantaneous short-term breakage of the extract protective film. The plot at 3.5% GPP concentration is more thermodynamically stable despite having a lower degree of passivation of the steel surface. This observation is due to the presence of more protonated GPP molecules available for inhibition of the corrosive species in the acid and prevention of their electrolytic transport to the steel surface. Secondly, the presence of more aggregate extract molecules possibly results in lateral among the excess extract molecules.

*Electrochemical impedance spectroscopy studies*

The electrochemical impedance characteristic of MS in 0.5M $H_2SO_4$ solution, without and with selected concentrations of GPP at room temperature is given in Fig. 3 in the form of (a) Nyquist and (b) Bode representations. In both the uninhibited and inhibited systems, the Nyquist diagrams exhibit a capacitive loop at the high to medium frequencies depicting the charged controlled corrosion process [21,28,33,65] and an inductive loop at the low frequencies which is associated with the relaxation of the corrosion products and/or adsorbed GPP molecules [52]. These two phenomena are also evident in the Bode graphs, for instance, the broadness of the Bode Phase in Fig. 3(b). Although the MS corroded in both the uninhibited and inhibited $H_2SO_4$ solutions, the influence of GPP on the corrosion process is very clear. In Fig. 3(a), the introduction of 1% GPP into the corrosive solution resulted in a noticeable increase in the diameter of the capacitive loop, meaning that the presence of GPP in the corrodent delayed the charge transfer process resulting in a decrease in the rate of corrosion of the metal [21,28,33,65]. The diameter of the capacitive loop (Fig. 3(a)) further increased, the Bode impedance modulus and Phase angle shifted toward nobler values as the concentration of GPP was raised to 3.5%. This implies that the corrosion inhibition performance of GPP is concentration dependent. A further inspection of the Nyquist graphs reveals that the capacitive loop

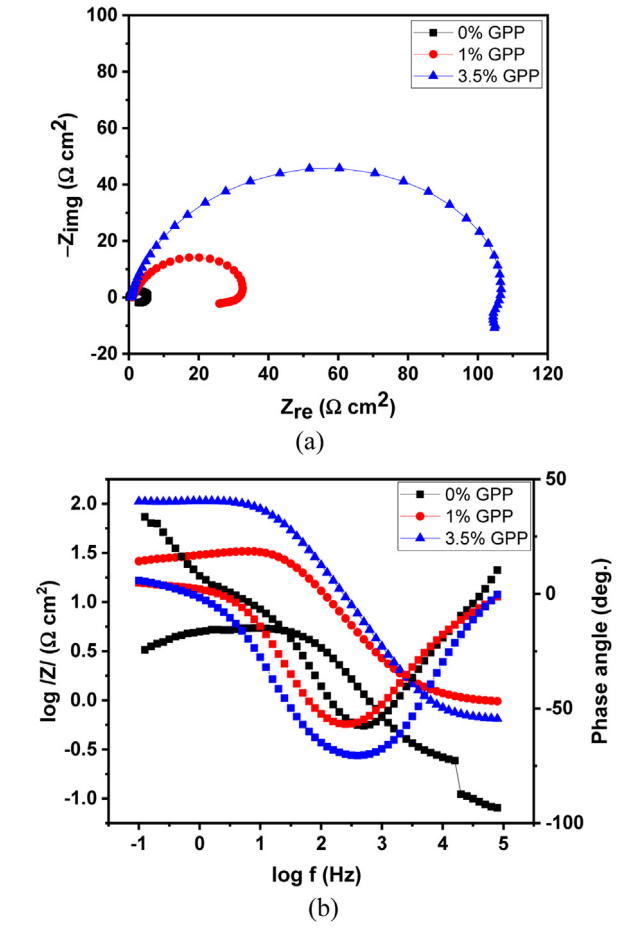


**Fig. 3.** Electrochemical impedance plots for MS corrosion in 0.5M $H_2SO4$ solution without and with selected concentrations of GPP at room temperature in (a) Nyquist and (b) Bode representations.

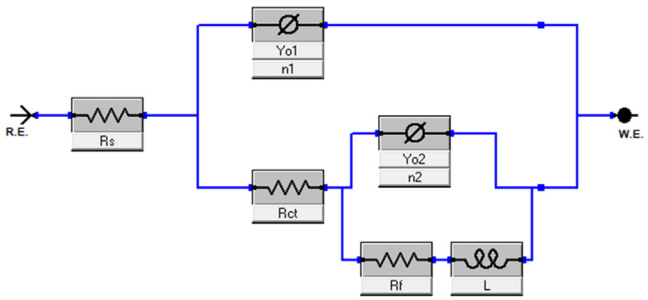


**Fig. 4.** Equivalent circuit used in the analysis of the electrochemical impedance data obtained for the corrosion of MS corrosion in 0.5M $H_2SO4$ solution without and with selected concentrations of GPP at room temperature.

is not a perfect circle which is a common feature of a solid electrode and describes the frequency dispersion caused by the heterogeneity of the working MS electrode [67]. The nature of the impedance spectra (Fig. 3) prompted the selection of the two-time constants equivalent circuit given in Fig. 4 to model the impedance data. The suitability of the selected equivalent circuit is reflected in the low fitting error and Chi square values given in Table 2. The elements of the equivalent circuit have the following meaning: $R_s$ = solution resistance), $R_{ct}$ = charge transfer resistance, Ø = constant phase element, $R_f$ = film resistance, and $R_L$ and L are the inductive elements. The use of Ø instead of a capacitor was necessitated by the imperfectness nature of the impedance [Fig. 3(a)] [32]. The impedance of Ø can be defined as [33]:

$$Z_{\emptyset} = \frac{1}{Y_0(jw)^n} \tag{6}$$

**Table 2**
Electrochemical impedance parameters for MS in 0.5M $H_2SO4$ solution without and with selected concentrations of GPP at 30°C

| | | $CPE_{dl}$± Er | | | |
|---|---|---|---|---|---|
| **Conc. (%)** | **$R_s$ ± Er (Ω cm²)** | **$Y_{01}$ (μΩ⁻¹ s² cm⁻²)** | **$n_1$** | **$R_{ct}$± Er (Ω cm²)** | **IE (%)** |
| 0 | 0.103±0.002 | 272.20±0.00 | 0.97±0.71 | 3.961±0.11 | - |
| 1 | 1.014±0.024 | 194.05±0.00 | 0.93±0.29 | 26.000±7.08 | 85 |
| 3.5 | 0.642±0.008 | 132.30±0.00 | 0.88±0.00 | 98.930±14.75 | 96 |

| $CPE_f$± Er | | | | | |
|---|---|---|---|---|---|
| **$Y_{02}$ (μΩ⁻¹ s² cm⁻²)** | **$n_2$** | **$R_f$± Er (Ω cm²)** | **$R_{total}$ (Ω cm²)** | **L (Ω s cm²)** | **$x^2$ (× $10^{-3}$)** |
| 127.90±0.00 | 0.99±0.05 | 0.441±0.112 | 4.402 | 3.97E-9 | 84.40 |
| 92.50±0.00 | 0.93±0.16 | 3.357±7.097 | 29.357 | 8.32E-4 | 5.60 |
| 82.00±0.00 | 0.63±0.11 | 0.388±0.007 | 99.318 | 4.86E-4 | 0.98 |

**Table 3**
Weight loss data for MS corrosion and GPP inhibition in 0.5 M $H_2SO_4$ solution at 240 h

| GPP Extract Concentration (%) | Weight Loss (g) | Corrosion Rate (mm/y) | Inhibition Efficiency (%) |
|---|---|---|---|
| 0 | 6.110 | 184.48 | - |
| 1 | 0.296 | 8.94 | 95.16 |
| 1.5 | 0.170 | 5.13 | 97.22 |
| 2 | 0.114 | 3.45 | 98.13 |
| 2.5 | 0.183 | 5.53 | 97.00 |
| 3 | 0.177 | 5.34 | 97.11 |
| 3.5 | 0.207 | 6.25 | 96.61 |

where $Y_0$ is the Ø constant, $n$ is the *CPE* exponent and describes the heterogeneity of the electrode, $j$ is an imaginary number, and $w$ the angular frequency in rad/s. The fitted values and the inhibition efficiency calculated using Equation 2 are given in Table 2.

$$IE(\%) = 1 - \frac{R_{total\ (blank)}}{R_{total\ (inhibited)}} \times 100 \tag{7}$$

In Table 2, both the $Y_{01}$ and $Y_{02}$ are seen to decrease with increase in the concentration of GPP. This is reflective of the improvement in the characteristics of the adsorbed steel surface film. Generally, $Y_0$ gives information about the characteristics of a metal surface film [62] and the smaller the $Y_0$ value, the better the surface film [27]. It does infer that the film formed due to GPP adsorption exhibited better protective properties than the corrosion product layer. This is also evident in the high value of the total charge resistance ($R_{total}$) obtained for the inhibited steel surface relative to the uninhibited (Table 2). By comparing the $Y_0$ and the $R_{total}$ values of the 1% and 3.5% GPP systems, it is seen that, an increase in the concentration of the GPP resulted in a further decrease in the $Y_0$ value and an increase in the $R_{total}$ value. Consequently, the 3.5% GPP exhibited inhibition efficiency of 96% relative to 85% exhibited by 1% GPP. The decrease in the $Y_0$ value and an increase in the $R_{total}$ value are caused by the increase in the thickness of the electrical double layer due to adsorption of the GPP molecules onto the steel surface [2]. It is also important to mention that the $n_1$ and $n_2$ values are very close to unity (Table 2). This shows that the MS/$H_2SO_4$ solution interface behaved as a capacitor [27].

*Weight loss analysis and optical microscopy*

Weight loss analysis of MS was done for 240 h at specific concentrations of GPP extract in 0.5 M $H_2SO_4$ solution. Data obtained from the analysis (weight loss, corrosion rate and inhibition efficiency) at 240 h of exposure are presented in Table 3. Fig. 5(a) and (b) shows the plots of corrosion rate of MS and inhibition efficiency of GPP versus exposure time from 24 h to 240 h. Optical images of MS before corrosion, after corrosion without GPP extract and after corrosion with GPP extract are shown in Fig 6. The plots in Fig. 5(a) shows the significant variation of MS corrosion rate at 0% GPP concentration and MS at 1%-3.5% GPP concentration. At 0% GPP concentration, MS being a ferrous alloy without passivating elements undergoes accelerated corrosion by single displacement due to the electrochemical action of $SO_4^{2-}$ anions in the electrolyte according to the equation below;

$$Fe_{(s)} + H_2SO_{4\ (aq)} \rightarrow FeSO_{4\ (aq)} + H_{2\ (g)} \tag{8}$$

Fe oxidize in the electrolyte by losing electrons and passing into the solution as $Fe^{2+}$ to form $FeSO_4$. $H_2$ gas is released through evolution mechanism resulting from the combination of H molecules. Between 24 h and 96 h, corrosion of MS increased progressively from 78.2 mm/y to 188.85 mm/y signifying increased reaction mechanism in the electrolyte. Beyond 96 h of exposure, corrosion rate of MS attained quasi stationary state before culminating at 184.48 mm/y (240 h). The

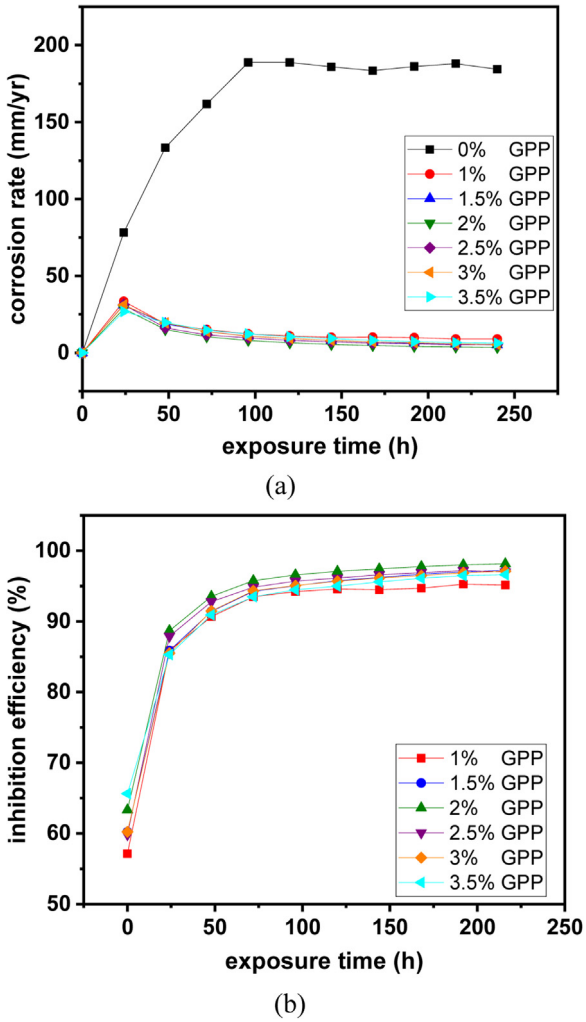


**Fig. 5.** (a) MS corrosion rate versus exposure time at 0%-3.5% GPP concentration and (b) GPP inhibition efficiency versus exposure time at 1%-3.5% GPP

image of MS (Fig. 6) at 240 h without GPP extracts showed a corroded morphology. Corrosion rate plots of MS at 1%-3.5% GPP concentration significantly decreased compared to the plot at 0% GPP concentration. This is due to inhibition effect of protonated GPP molecules which effectively suppressed the corrosion reaction processes occurring on MS surface in the electrolyte and alteration of the corrosive electrolyte. Taking into consideration, the similar plot configuration of MS corrosion rate in the presence of GPP extract, it can be deduced, that increase in GPP concentration, despite significantly reducing the corrosion rate of MS has minimal influence on the corrosion behavior of MS. In the presence of the extracts, corrosion rate of MS initiated at values between 26.87 mm/y and 33.51 mm/y. The plot shows the corrosion rate decreased progressively with time signifying time dependent suppression effect of the extract molecules whereby the anions of the corrosion species are inhibited from getting to MS surface. Relative stability was attained at 144 h where corrosion rate of MS varies between 5.44 mm/y and 10.06 mm/y. At 240 h, corrosion rate has marginally decreased to values between 3.451 mm/y and 8.937 mm/y. The image for MS corrosion in the presence of GPP extract (Fig. 2) shows the presence of GPP extract film which stifled the corrosion rate reactions on the steel surface. Observation of the inhibition efficiency values in Table 2 shows the final values at 240 h. The values varied from 95.16% at 1% GPP concentration to 98.13% at 2% GPP concentration confirming that GPP protection performance is independent of its concentration. Variation of inhibition efficiency with respect to time shows in Fig. 5(b) shows at 24 h inhibition efficiency varied between 57.14% and 65.64% before progressing to final values shown in Table 3.

*ATF-FTIR Spectroscopy Studies*

To further prove the adsorption of GPP on MS surface leading to the suppression of corrosion in the studied corrosive medium, the FTIR spectra of the crude GPP and the film extracted from the MS surface after corrosion were compared as

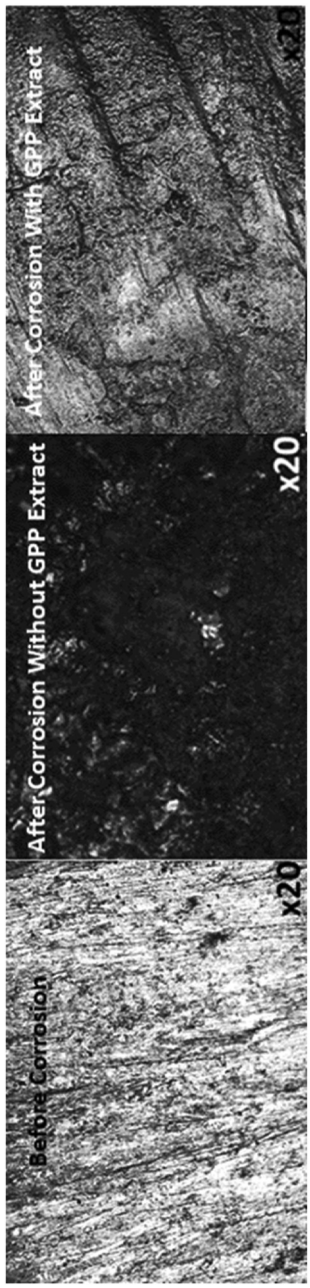


**Fig. 6.** Optical images of MS

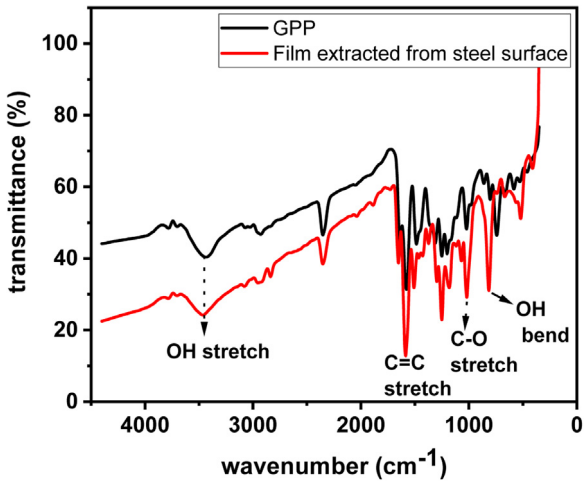


**Fig. 7.** The FTIR spectra of the raw GPP (mixture of Ginger and Grape fruit oils) and the film extracted from the high carbon steel surface after immersion in 0.5M $H_2SO_4$ solution containing 3.5% GPP at room temperature.

shown in Fig. 7. In the GPP spectrum, the prominent absorption bands are at 3450 $cm^{-1}$, 2390 $cm^{-1}$, 1610 $cm^{-1}$, 1250 $cm^{-1}$, 1020 $cm^{-1}$, and 770 $cm^{-1}$. The broad band at 3450 $cm^{-1}$ is assigned to O-H stretch and the band at 1610 $cm^{-1}$ is due to the conjugated C=C stretching [49]. The absorption band at 1020 $cm^{-1}$ is consistent with the C-O stretching of a primary alcohol [58] and the band at 770 $cm^{-1}$ is associated with the alcohol, OH out-of-plane bending. This result, as expected show that the essential oils contained multiple organic compounds. Although the compositions and constituents of essential oils may vary depending on the geochemistry of the soil where it is cultivated, it is generally made up of terpenes such as terpineol, cineole, citronellal, and others [9]. Compared to the GPP, the spectrum of the extracted film exhibits all the absorption bands noted in the GPP spectrum. This provides experimental evidence to the claim of GPP molecules adsorption on the steel surface, which in extension is responsible for the inhibition of the metal against corrosion. Furthermore, it is observed that the C=C, C-O stretching, and the OH out-of-plane bending bands are sharper and more prominent in the extracted film spectrum relative to the raw GPP spectrum. This is suggestive of the involvement of these functional groups in the bonding process [29].

## Conclusion

Admixture of ginger and grapefruit essential oil effectively inhibited mild steel corrosion in dilute $H_2SO_4$ solution. ATF-FTIR data showed the oils contains multiple organic compounds and the corresponding spectrum of the extracted film GPP molecules adsorbed on the steel surface proves it is responsible for the inhibition of the metal against corrosion. Open circuit potential plots of the inhibited steel were significantly more electropositive relative to the plot without the oil extract. Passivation of the steel in the presence of the extract significantly altered the dynamics of the corrosion reaction processes. Results from Potentiodynamic polarization and weight loss analysis confirmed the effective inhibition properties of the oil extract with inhibition efficiency generally above 90%.

## Declaration of Competing Interest

No conflict of interest exists.

## Acknowledgment

The author appreciates the support of Covenant University towards the successful actualization of this research.

## References

[1] Z. Ahmad, Selection of materials for corrosive environment, Principles of Corrosion Engineering and Corrosion Control, Elsevier Ltd, 2006, doi:10.1016/B978-0-7506-5924-6.X5000-4.
[2] M.T. Alhaffar, S.A. Umoren, I.B. Obot, A.A. IB Shaikh, M.M Solomon, Studies of the anticorrosion property of a newly synthesized Green isoxazolidine for API 5L X60 steel in acid environment, J. Mater. Res. Technol. 8 (2019) 4399–4416.
[3] H. Ashassi-Sorkhabi, M.R. Majidi, K. Seyyedi, Investigation of inhibition effect of some amino acids against steel corrosion in HCl solution, Appl. Surf. Sci. 225 (2004) 176–185.
[4] H. Ashassi-Sorkhabi, B. Masoumi, P.E. Ejbari, Corrosion inhibition of mild steel in acidic media by basic yellow 13 dye, J. Appl. Electrochem. 39 (9) (2009) 1497–1501.

[5] Bahlakeh, M. Ramezanzadeh, B Ramezanzadeh, Experimental and theoretical studies of the synergistic inhibition effects between the plant leaves extract (PLE) and zinc salt (ZS) in corrosion control of carbon steel in chloride solution, J. Mol. Liq. 248 (2017) 854–870.
[6] A. Batah, M. Belkhaouda, L. Bammou, A. Anejjar, R. Salghi, A. Chetouani, L. Bazzi, B. B. Hammouti, Corrosion inhibition of carbon steel in acidic medium by Grapefruit oil extract, Mor. J. Chem. 5 (4) (2017), doi:10.48317/IMIST.PRSM/morjchem-v5i4.9797.
[7] A. Berradja, Electrochemical techniques for corrosion and tribocorrosion monitoring: fundamentals of electrolytic corrosion, in: A Singh (Ed.), Corrosion Inhibitors, IntechOpen, London, 2019, doi:10.5772/intechopen.85392.
[8] K. Boumhara, M. Tabyaoui, C. Jama, F Bentiss, Artemisia Mesatlantica essential oil as green inhibitor for carbon steel corrosion in 1 M HCl solution: Electrochemical and XPS investigations, J. Ind. Eng. Chem. 29 (2015) 146–155.
[9] H. Boughendjioua, N.E.H. Mezedjeri, I. Idjouadiene, Chemical constituents of Algerian mandarin (Citrus reticulata) essential oil by GC-MS and FT-IR analysis, Curr. Issues Pharm. Med. Sci. 33 (2020) 197–201.
[10] M. Bouoidina, A. Chaouch, A. Abdellaoui, B. Lahkimi, F. Hammouti, M. El-Hajjaji, A. Taleb, A. Nahle, Essential oil of "Foeniculum vulgare": antioxidant and corrosion inhibitor on mild steel immersed in hydrochloric medium, Anti-Corros. Method M. 64 (5) (2017) 563–572.
[11] W.D. Collins, R.E. Weyers, I.L. Al-Qadi, Chemical treatment of corroding steel reinforcement after removal of chloride-contaminated concrete, NACE Corros. 49 (1) (1993) 74–88.
[12] G.C. Dariva, A.F. Alexandre, Corrosion inhibitors–principles, mechanisms and applications, developments in corrosion protection, Intechopen (2014) 365–379, doi:10.5772/57255.
[13] A. Dehghani, G. Bahlakeh, B. Ramezanzadeh, M. Ramezanzadeh, Electronic/atomic level fundamental theoretical evaluations combined with electrochemical/surface examinations of Tamarindus indiaca aqueous extract as a new green inhibitor for mild steel in acidic solution (HCl 1 M), J. Taiwan Inst. Chem. E. 102 (2019) 349–377.
[14] A. Dehghani, F. Poshtiban, G. Bahlakeh, B. Ramezanzadeh, Fabrication of metal-organic based complex film based on three-valent samarium ions-[bis (phosphonomethyl) amino] methylphosphonic acid (ATMP) for effective corrosion inhibition of mild steel in simulated seawater, Constr. Build. Mater. 239 (117812) (2020).
[15] G. Dehghani, G. Bahlakeh, Ramezanzadeh, Green Eucalyptus leaf extract: A potent source of bio-active corrosion inhibitors for mild steel, Bioelectrochemistry 130 (107339) (2019).
[16] D. Dwivedi, K. Lepkov, T. Becker, Carbon steel corrosion: A review of key surface properties and characterization methods, RSC Adv. 7 (2017) 4580–4610.
[17] U.J. Ekpe, U.J. Ibok, B.I. Ita, O.E. Offiong, E.E. Ebenso, Inhibitory action of methyl and phenylthiosemicarbazone derivatives on the corrosion of mild steel in hydrochloric acid, Mater. Chem. Phys. 40 (1995) 87–93.
[18] Y. El Ouadi, A. Bouyanzer, L. Majidi, J. Paolini, J.M. Desjobert, J. Costa, A. Chetouani, B. Hammouti, Salvia officinalis essential oil and the extract as green corrosion inhibitor of mild steel in hydrochloric acid, J. Chem. Pharm. Res. 6 (7) (2014) 1401–1416.
[19] E. El Ouariachi, A. Bouyanzer, R. Salghi, B. Hammouti, J.M. Desjobert, J. Costa, J. Paolini, L. Majidi, Inhibition of corrosion of mild steel in 1 M HCl by the essential oil or solvent extracts of Ptychotis verticillata, Res. Chem. Intermed. 41 (2015) 935–946.
[20] B.R. Fazal, T. Becker, B. Kinsella, K. Lepkova, A review of plant extracts as green corrosion inhibitors for $CO_2$ corrosion of carbon steel, npj Mater. Degrad. 6 (5) (2022).
[21] P. Feng, K. Wan, G. Cai, L. Yang, Y Li, Synergistic protective effect of carboxymethyl chitosan and cathodic protection of X70 pipeline steel in seawater, RSC Adv. 7 (2017) 3419–3427.
[22] A. Fidrusli, Suryanto, M Mahmood, Ginger extract as green corrosion inhibitor of mild steel in hydrochloric acid solution, IOP Conf. Ser.: Mater. Sci. Eng. 290 (2018) 012087, doi:10.1088/1757-899X/290/1/012087.
[23] A.S. Fouda, A.A. Nazeer, M. Ibrahim, M. Fakih, Ginger extract as green corrosion inhibitor for steel in sulfide polluted salt water, J. Kor. Chem. Soc. 57 (2) (2013) 272–278, doi:10.5012/jkcs.2013.57.2.272.
[24] S. Fu, L. Li, Y. Cao, L. Wang, L. Yan, L. Lu, Tryptophan as green corrosion inhibitor for low carbon steel in hydrochloric acid solution, J. Mater. Sci. 45 (2010) 979–986.
[25] H.S. Gadow, M.M. Motawea, Investigation of the corrosion inhibition of carbon steel in hydrochloric acid solution by using ginger roots extract, RCS Adv. 40 (7) (2017) 24576–24588.
[26] F. García-Labiano, L.F. de Diego, A. Cabello, P. Gayán, A. Abad, J. Adánez, G. Sprachmann, Sulphuric acid production via Chemical Looping Combustion of elemental Sulphur, Appl. Energy 178 (2016) 736–745, doi:10.1016/j.apenergy.2016.06.110.
[27] H. Gerengi, N. Sen, I. Uygur, M.M. Solomon, Corrosion response of ultra-high strength steels used for automotive applications, Mater. Res. Express. 6 (0865a6) (2019), doi:10.1088/2053-1591/ab2178.
[28] Z. Ghazi, H. Elmssellem, M. Ramdani, A. Chetouani, R. Rmil, A. Aouniti, C. Jama, B. Hammouti, Corrosion inhibition by naturally occurring substance containing Opuntia-Ficus Indica extract on the corrosion of steel in hydrochloric acid, J. Chem. Pharm. Res. 6 (2014) 1417–1425.
[29] S.A. Haladu, S.A. Umoren, S.A. Ali, M.M. Solomon, A-R.I. Mohamed, Synthesis, characterization and electrochemical evaluation of anticorrosion property of a tetrapolymer for carbon steel in strong acid media, Chin. J. Chem. Eng. (2019) 965–978.
[30] E. Hamdani, O. El Ouariachi, A. Mokhtari, N. Salhi, B. Chahboun, A. ElMahi, A. Bouyanzer, B. Zarrouk, J. Hammouti, Costa, Chemical constituents and corrosion inhibition of mild steel by the essential oil of Thymus algeriensis in 1.0 M hydrochloric acid solution, Der. Pharm. Chem. 7 (8) (2015) 252–264.
[31] S.M.Z. Hossain, S.A. Razzak, M.M. Hossain, Application of essential oils as green corrosion inhibitors, Arab. J. Sci. Eng. 45 (2020) 7137–7159.
[32] C.H. Hsu, F. Mansfeld, Concerning the conversion of the constant phase element parameter $Y_0$ into a capacitance, Corrosion 57 (9) (2001) 747–748.
[33] Y. Jiang, Y. Liu, S. Gao, X. Guo, J. Zhang, Experimental and theoretical studies on corrosion inhibition behavior of three imidazolium-based ionic liquids for magnesium alloys in sodium chloride solution, J. Mol. Liq. (116998) (2022) 345.
[34] F.S. Kadhim, Investigation of carbon steel corrosion in water base drilling mud, Mod. Appl. Sci. 5 (1) (2011).
[35] L. Khaksar, J. Shirokoff, Effect of elemental sulfur and sulfide on the corrosion behavior of Cr-Mo low alloy steel for tubing and tubular components in oil and gas industry, Materials 10 (2017) 430.
[36] Y.I. Kuznetsov, Organic inhibitors of corrosion of metals, Springer US, 1996, doi:10.1007/978-1-4899-1956-4.
[37] A. Lahhit, J.M. Bouyanzer, B. Desjobert, R. Hammouti, J. Salghi, C. Costa, F. Jama, Bentiss, L Majidi, Fennel (Foeniculum Vulgare) essential oil as green corrosion inhibitor of carbon steel in hydrochloric acid solution, Port. Electrochim. Acta. 29 (2) (2011) 127–138.
[38] Y. Li, P. Zhao, Q. Liang, B. Hou, Berberine as a natural source inhibitor for mild steel in 1 M $H_2SO_4$, Appl. Surf. Sci. 252 (2005) 1245–1253.
[39] G.Q. Liu, Z.Y. Zhu, W. Ke, C.I. Han, C.L. Zeng, Corrosion behavior of stainless steels and nickel-based alloys in acetic acid solutions containing bromide ions, NACE Corros. 57 (8) (2001) 730–738.
[40] R.T. Loto, C.A. Loto, Effect of P-phenylediamine on the corrosion of austenitic stainless steel type 304 in hydrochloric acid, Int. J. Elect. Sci. 7 (10) (2012) 9423–9440.
[41] R.T. Loto, Comparative study of the pitting corrosion resistance, passivation behavior and metastable pitting activity of NO7718, NO7208 and 439L super alloys in chloride/sulphate media, J. Mater. Res. Techn. 8 (1) (2019) 623–629.
[42] R.T. Loto, Corrosion inhibition studies of the combined admixture of 1,3-diphenyl-2-thiourea and 4-hydroxy-3-methoxybenzaldehyde on mild steel in dilute acid media, Rev. Colomb. Quim. 46 (1) (2017) 20–32.
[43] R.T. Loto, Study of the synergistic effect of 2-methoxy-4-formylphenol and sodium molybdenum oxide on the corrosion inhibition of 3CR12 ferritic steel in dilute sulphuric acid, Result. Phys. 7 (2017) 769–776.
[44] C.A. Loto, R.T. Loto, O.O. Joseph, A.P.I. Popoola, Corrosion inhibitive behaviour of camellia sinensis on aluminium alloy in $H_2SO_4$, Int. J. Elect. Sci. 9 (3) (2014) 1221–1231.

[45] R.T. Loto, R. Leramo, B. Oyebade, Synergistic combination effect of salvia officinalis and lavandula officinalis on the corrosion inhibition of low-carbon steel in the presence of $SO_4^{2-}$ and $Cl^-$ containing aqueous environment, J. Fail. Anal. & Preven. 18 (6) (2018) 1429–1438.
[46] N. Mohanan, Palaniswamy, Corrosion inhibition of mild steel by ethanolic extracts of Ricinus communis leaves, Indian J. Chem. Technol. 12 (2005) 356–360.
[47] Monticelli, Corrosion Inhibitors, in: Klaus Wandelt (Ed.), Encyclopedia of Interfacial Chemistry, Elsevier, Amsterdam, 2018, pp. 164–171, doi:10.1016/B978-0-12-409547-2.13443-2.
[48] H. Müller, in: Sulfuric Acid and Sulfur Trioxide" in Ullmann's Encyclopedia of Industrial Chemistry, Wiley-VCH, Weinheim, 2000, p. 2000, doi:10.1002/14356007.a25_635.
[49] A.B.D. Nandiyanto, R. Oktiani, R. Ragadhita, How to read and interpret FTIR spectroscope of organic material, Indones. J. Sci. Technol. 4 (2019) 97–118.
[50] J. Narenkumar, P. Parthipan, A.U.R. Nanthini, G. Benelli, K. Murugan, A. Rajasekar, Ginger extract as green biocide to control microbial corrosion of mild steel, 3 Biotech. 7 (2) (2017) 133, doi:10.1007/s13205-017-0783-9.
[51] ÖZcan, AC impedance measurements of cysteine adsorption at mild steel/sulphuric acid interface as corrosion inhibitor, J. Solid State Electrochem. 12 (2008) 1653–1661.
[52] M. Palomar-Pardavé, M. Romero-Romo, H. Herrera-Hernández, M.A. Abreu-Quijano, N.V. Likhanova, J. Uruchurtu, J.M. Juárez-García, Influence of the alkyl chain length of 2 amino 5 alkyl 1, 3, 4 thiadiazole compounds on the corrosion inhibition of steel immersed in sulfuric acid solutions, Corros. Sci. 54 (2012) 231–243.
[53] J.C. Philip, in: Survey of Industrial Chemistry, John Wiley & Sons, New York, 1987, pp. 45–57.
[54] F. Presuel-Moreno, M.A. Jakab, N. Tailleart, M. Goldman, J.R. Scully, Corrosion-resistant metallic coatings, Mater. Today. 11 (10) (2008) 14–23.
[55] G. Quartarone, L. Ronchin, A. Vavasori, C. Tortato, L. Bonaldo, Inhibitive action of gramine towards corrosion of mild steel in deaerated 1.0 M hydrochloric acid solutions, Corros. Sci. 64 (2012) 82–89.
[56] M. Ramezanzadeh, Z. Sanaei, G. Bahlakeh, B. Ramezanzadeh, Highly effective inhibition of mild steel corrosion in 3.5% NaCl solution by green Nettle leaves extract and synergistic effect of eco-friendly cerium nitrate additive: Experimental, MD simulation and QM investigations, J. Mol. Liq. 256 (2018) 67–83.
[57] L.M. Rivera-Grau, M. Casales, I. Regla, D.M. Ortega-Toledo, J.A. Ascencio-Gutierrez, J. Porcayo-Calderon, L. Martinez-Gomez, Effect of organic corrosion inhibitors on the corrosion performance of 1018 carbon steel in 3% NaCl solution, Int. J. Elect. Sci. 8 (2013) 2491–2503.
[58] T.S.T. Saharuddin, L.N. Ozair, A.S. Zulkifli, N.S.H. Shah, N.S. Sahidan, Characterization of encapsulated ginger essential oils and its antimicrobial properties, J. Acad. (2020) 1–6.
[59] M.S. Sanusi, S.R. Shamsudin, A. Rahmat, R. Wardan, Electrochemical corrosion behaviours of AISI 304 austenitic stainless steel in NaCl solutions at different pH, AIP Conf. Proc. 2030 (020116) (2018).
[60] Saratha, N. Kasthuri, P. Thilagavathy, Environment friendly acid corrosion inhibition of mild steel by Ricinus communis leaves, Der. Pharma. Chem. 1 (2) (2009) 249–257.
[61] R.A.L. Sathiyanathan, M.M. Essa, S. Maruthamuthu, M. Selvanayagam, N. Palaniswamy, Inhibitory effect of Ricinus communis (Castor-oil plant) leaf extract on corrosion of mild steel in low chloride medium, J. Indian Chem. Soc. 82 (4) (2005) 357–359.
[62] J.Y. Sha, H.H. Ge, C. Wan, L-T. Wang, S-Y. Xie, X-J. Meng, Y-Z. Zhao, Corrosion inhibition behaviour of sodium dodecyl benzene sulphonate for brass in an $Al_2O_3$ nanofluid and simulated cooling water, Corros. Sci. 148 (2019) 123–133.
[63] D.D.N. Singh, T.B. Singh, B. Gaur, The role of metal cations in improving the inhibitive performance of hexamine on the corrosion of steel in hydrochloric acid solution, Corros. Sci. 37 (6) (1995) 1005–1019.
[64] H. Venzlaff, D. Enning, J. Srinivasan, K.J.J. Mayrhofer, A.W. Hassel, F. Widdel, M. Stratmann, Accelerated cathodic reaction in microbial corrosion of iron due to direct electron uptake by sulfate-reducing bacteria, Corros. Sci. 66 (2013) 88–96.
[65] C. Wang, C. Zou, Y. Cao, Electrochemical and isothermal adsorption studies on corrosion inhibition performance of $\beta$-cyclodextrin grafted polyacrylamide for X80 steel in oil and gas production, J. Mol. Struct. 1228 (129737) (2021).
[66] D.A. Winkler, Predicting the performance of organic corrosion inhibitors, Metals 7 (12) (2017) 553, doi:10.3390/met7120553.
[67] N. Yilmaz, A. Fitoz, U. Ergun, K.C. Emregul, A combined electrochemical and theoretical study into the effect of 2-((thiazole-2-ylimino)methyl)phenol as a corrosion inhibitor for mild steel in a highly acidic environment, Corros. Sci. 111 (2016) 110–120.
[68] M. Znini, Application of essential oils as green corrosion inhibitors for metals and alloys in different aggressive mediums - a review, Arab. J. Med. Aromat. Plant. 3 (5) (2019).
[69] M. Bathily, B. Ngom, D. Gassama, S. Tamba, Review on essential oils and their corrosion-inhibiting properties, Am. J. Appl. Chem. 9 (3) (2021) 65–73.